Biogeosciences Discuss., 10, 4331–4365, 2013
www.biogeosciences-discuss.net/10/4331/2013/
doi:10.5194/bgd-10-4331-2013

Biogeosciences Discussions
Open Access

Synergistic effects of pCO_2 and iron availability on nutrient consumption ratio of the Bering Sea phytoplankton community

K. Sugie[1,2], H. Endo[3], K. Suzuki[2,3], J. Nishioka[4], H. Kiyosawa[5], and T. Yoshimura[1]

[1]Environmental Science Research Laboratory, Central Research Institute of Electric Power Industry, 1646 Abiko, Abiko, Chiba 270-1194, Japan
[2]Faculty of Environmental Earth Science, Hokkaido University and CREST-JST, North 10 West 5, Kita-ku, Sapporo, Hokkaido 060-0810, Japan
[3]Graduate School of Environmental Science, Hokkaido University, North 10 West 5, Kita-ku, Sapporo, Hokkaido 060-0810, Japan
[4]Pan-Okhotsk Research Center, Institute of Low Temperature Science, Hokkaido University, North 19 West 8, Kita-ku, Sapporo, Hokkaido 060-0819, Japan
[5]Marine Biological Research Institute of Japan, 4–3–16, Toyomachi, Shinagawa-ku, Tokyo, 142–0042, Japan

Received: 22 January 2013 – Accepted: 20 February 2013 – Published: 6 March 2013

Correspondence to: K. Sugie (kojisugie@gmail.com)

Published by Copernicus Publications on behalf of the European Geosciences Union.

BGD
10, 4331–4365, 2013

Abstract

Little is known concerning the effect of CO_2 on phytoplankton ecophysiological processes under nutrient and trace element-limited conditions, because most of the CO_2 manipulation experiments have been conducted under these element-replete conditions. To investigate the effects of CO_2 and iron availability on phytoplankton ecophysiology, we conducted an experiment using a phytoplankton community in the iron-limited, high-nutrient, low-chlorophyll (HNLC) region of the Bering Sea basin in September 2009. Carbonate chemistry was controlled by the bubbling of the several levels of CO_2 concentration (180, 380, 600, and 1000 ppm) controlled air, and two iron conditions were established with or without the addition of inorganic iron. We demonstrated that in the iron-limited control conditions, the specific growth rate and the maximum photochemical quantum efficiency (F_v/F_m) of photosystem (PS) II decreased with increasing CO_2 levels, suggesting a further decrease in iron bioavailability under the high CO_2 conditions. In addition, biogenic silica to particulate nitrogen and biogenic silica to particulate organic carbon ratios increased from 2.65 to 3.75 and 0.39 to 0.50, respectively with an increase in CO_2 level in the iron-limited controls. In contrast, in the iron-added treatments, specific growth rate, F_v/F_m values and elemental compositions did not change in response to the CO_2 variations, indicating that the addition of iron cancelled out the effect of the modulation of iron bioavailability due to the change in carbonate chemistry. Our results suggest that high CO_2 conditions can alter the biogeochemical cycling of nutrients through decreasing iron bioavailability in the iron-limited HNLC regions in the future.

1 Introduction

Marine phytoplankton production and their elemental compositions play a crucial role in driving ocean biogeochemical cycling of nutrients (Redfield et al., 1963). The elemental composition of phytoplankton is affected by changing ambient conditions such

BGD
10, 4331–4365, 2013

as nutrient concentrations and partial pressure of CO_2 (pCO_2) (e.g., Takeda, 1998; Burkhardt et al., 1999; Kudo, 2003), and difference in community compositions (Arrigo et al., 1999; Sugie et al., 2010a). This evidence suggests that the biogeochemical cycling of nutrients can change in response to future global climate change (Hutchins et al., 2009). Therefore, the factors modulating nutrient biogeochemistry are important issues to understand and to better prediction future environment under climate change.

Anthropogenic CO_2 emission through burning fossil fuels and land use change causes an increase in atmospheric CO_2 concentrations, which leads to an increase in the seawater CO_2 level in the global surface ocean (Caldeira and Wickett, 2005). As more anthropogenic CO_2 dissolves into the seawater, the surface ocean acidity will concomitantly increase further, which causes ocean acidification (Raven et al., 2005). It has been reported that the ocean acidification affects the elemental composition of phytoplankton, suggesting that oceanic nutrient biogeochemistry will alter according to future high-CO_2 conditions (Hutchins et al., 2009). However, most of the previous studies concerning the effect of CO_2 on phytoplankton ecophysiological processes were conducted under nutrient and trace element-replete conditions. There is a distinct lack of knowledge regarding the effect of CO_2 on phytoplankton ecophysiology under nutrient or trace element-limited conditions, despite the fact that the phytoplankton production in oceanic environments is often limited to at least one element such as nitrogen and iron (Saito et al., 2008).

Iron availability also affects the elemental composition of phytoplankton (Takeda, 1998; Sugie et al., 2010a), because iron plays key roles in their metabolic processes such as photosynthesis, respiration, and nitrate and nitrite assimilations (Raven et al., 1999). Phytoplankton productivity, specifically that of diatoms with a relatively large-cell size, is limited by iron availability in a large area of the oceans, which is called high nutrient, low chlorophyll (HNLC) region (e.g., de Baar et al., 2005). Recent studies reported that iron availability will change through increasing the contribution of ferrous to ferric iron (Millero et al., 2009) and conditional stability constant of iron-ligand complex (Shi et al., 2010) in response to the increase in the acidity of seawater. Other human

BGD
10, 4331–4365, 2013

perturbations such as land use and SO_2 and NO_x emissions will also alter the iron distribution and bioavailability in the open oceans (Mahowald et al., 2009). Therefore, the interactive effects of the ocean acidification and the iron availability will be expected to play crucial roles in the biogeochemical cycling of nutrients in the HNLC regions. Previous CO_2 manipulation studies using Southern Ocean and western subarctic Pacific phytoplankton communities suggest that the elemental composition or nutrient drawdown ratio was not affected by CO_2 variations under iron-limited conditions (Feng et al., 2010; Endo et al., 2013). In contrast, the elemental composition of unialgal culture of *Pseudo-nitzschia pseudodelicatissima* changed in response to the change in both CO_2 levels and bioavailable dissolved inorganic iron concentrations (Sugie and Yoshimura, 2013). Further information is still required concerning the interactive effects of iron and ocean acidification on the elemental composition of phytoplankton to better understand the future biogeochemistry of nutrients in high CO_2 oceans.

In the present study, we conducted a CO_2 and iron manipulation study using Bering Sea phytoplankton community. The central Bering Sea basin is one of the precise ecosystems for investigating the effects of CO_2 and iron, because the region is characterized as an iron-limited HNLC region (Leblanc et al., 2005). However, to date, no bioassays for either CO_2 or iron manipulation experiment have been conducted in the region. Here, we demonstrate the effects of CO_2 and iron on the net growth rate, the photochemistry of photosystem (PS) II, the species composition and the elemental composition of phytoplankton. Specifically, we examined these effects on diatoms, which is a key component of carbon and nutrient biogeochemistry especially for silicon.

2 Materials and methods

2.1 Sampling location

Seawater for the incubation experiment was collected in the Bering Sea (53° 05′ N, 177° 00′ W) on 9 September 2009, aboard the R/V *Hakuho-Maru* (JAMSTEC), during

BGD
10, 4331–4365, 2013

the KH09-4 cruise (Fig. 1). At the sampling station, surface temperature, salinity, and mixed layer depth were 8.2 °C, 33.10, and ~ 40 m, respectively. The mixed layer depth was estimated from the first downward increase in $\sigma t \geq 0.02\,m^{-1}$.

2.2 Incubation experiment

Approximately 300 L of seawater were collected at 10 m depth using acid-cleaned Teflon-coated 10 L Niskin-X sampling bottles (General Oceanics) attached to a CTD-CMS. Seawater for the experiment was sieved by 197 µm acid-cleaned Teflon-mesh to eliminate mesozooplankton, and the prescreened seawater was poured into six acid-washed 50 L polypropylene tanks to homogenize seawater samples. The two tanks were used for iron-limited conditions (controls). Inorganic iron stock solution was added to four tanks to make the final concentration of 5 nmol L^{-1} (Fe-added treatments), and then the seawater samples were mixed thoroughly but gently. Then, the seawater was dispensed into triplicate 12 L polycarbonate incubation bottles per 50 L tank. Carbonate chemistry was manipulated by injecting CO_2 concentration (xCO_2) controlled dry-air (Nissan Tanaka Corp., Saitama, Japan) directly into the incubation bottles at a flow rate of 100 mL per minute for the first 24 h and, thereafter, maintained at 50 mL per minute during the culture experiment (Yoshimura et al., 2010). The xCO_2 of the injected air was set at 380 and 600 ppm for controls (hereafter C-380 and C-600, respectively) and 180, 380, 600, and 1000 ppm for Fe-added treatments (hereafter Fe-180, Fe-380, Fe-600, and Fe-1000, respectively). The injected air was passed through a 0.2 µm in-line filter to avoid trace element contaminations from gas cylinders and lines for all bottles. The dissolved inorganic carbon (DIC) and total alkalinity (TA) were measured periodically to calculate carbonate chemistry (see below). Incubations lasted for 7 days in an on-deck incubator. Temperature of the incubator was maintained at near-ambient sea surface temperature (~ 8 °C) by a constant temperature water circulator (Yamato Scientific Co., Ltd.). The incubator was covered with neutral density mesh to decrease surface irradiance to 50 %. Photon flux was measured using a 4π quantum sensor in combination with a data logger (JFE Advantech Co., Ltd.).

BGD
10, 4331–4365, 2013

Samples for size fractionated (10 µm and GF/F) Chl *a* and nutrients were collected daily. Similarly, samples for particulate organic carbon (POC), particulate nitrogen (PN), biogenic silica (BSi), DIC, TA, microscopic observation, and the maximum photochemical quantum yield (F_v/F_m) of PS II for phytoplankton were collected at days 1.9, 3.6, and 5.7 for the iron-limited controls (hereafter day 2, 4, and 6, respectively) and at days 1.9, 2.6, 4.7, and 6.6 for the iron-added treatments (hereafter day 2, 3, 5, and 7, respectively). Samples for total dissolvable Fe (TD-Fe, unfiltered) and dissolved Fe (D-Fe, < 0.22 m) at the beginning of the experiment were collected directly from the spigot of the Niskin-X sampling bottles, using 0.22 µm cartridge filter (Merck Millipore) with gravity filtration for D-Fe. At the end of the experiment, TD-Fe samples were collected from the incubation bottles. Size fractionated Chl *a* samples were collected sequentially on the 10 µm pore size of polycarbonate filter (Whatman) without vacuum and on GF/F filter (Whatman) under gentle vacuum at < 100 mm Hg. Filter samples for Chl *a* were extracted with *N*,*N*-dimethylformamide immediately after the filtration and stored at −20 °C in the dark at least 24 h until aboard analysis (Suzuki and Ishimaru, 1990). Samples for POC and PN were collected on a pre-combusted (450 °C, 4 h) GF/F filter. Samples for BSi were collected on the 0.4 µm pore size of polycarbonate membrane filter under gentle vacuum. Samples for POC, PN, BSi, and nutrients were stored at −20 °C until analysis on a land laboratory. The DIC and TA samples were collected into gas-tight glass vials and poisoned with $HgCl_2$ prior to the storage at 4 °C for on-land analysis. For microscopic analysis, Lugol's acidic iodine solution was added to seawater (4 % final volume). For iron analysis, seawater samples were acidified at pH 3.2 with 10 mol L^{-1} formic acid and 2.4 mol L^{-1} ammonium formate buffer after the sample collection and stored for several months at room temperature until analysis.

To examine the silicification of the diatom cells, we conducted incubations using 2-(4-pyridyl)-5-((4-(2-dimethylaminoethyl-aminocarbamoyl)-methoxy)phenyl)oxazole (PDMPO) fluorescence probe (Life Technologies Corp.), which incorporates and stains newly deposited diatom frustules during their growth (Leblanc and Hutchins, 2005; Ichinomiya et al., 2010). We used the fluorescence intensity of the PDMPO within the

BGD
10, 4331–4365, 2013

frustule as an index of silicification of the diatom cells under different CO_2 and iron conditions. Seawater samples for PDMPO labeling incubation were collected from the 12 L polycarbonate incubation bottles by siphon and dispensed into acid-cleaned 170 mL polycarbonate bottles without head space. Triplicate 170 mL incubation bottles were prepared for each treatment. The PDMPO incubation was started on day 3.3 of the iron-limited control treatments and day 2.3 of the Fe-added treatments, when macronutrients were not exhausted. The PDMPO stock solution (1 mmol L^{-1}) was added to the 170 mL incubation bottles to make 0.25 µmol L^{-1} (Leblanc and Hutchins, 2005). The bottles were incubated for 24 h in the onboard incubator. After the incubation, seawater samples were filtered onto black-stained 0.4 µm polycarbonate filters and mounted on glass slide with immersion oil. The glass slide was stored at −20 °C until on-land microscopic observation and digital image analysis. Chl *a* samples were collected on GF/F filter at the end of the PDMPO incubations to compare the growth of phytoplankton between the 170 mL and 12 L incubation bottles. Unfortunately, we were not able to measure carbonate chemistry during the PDMPO experiment due to a water volume limitation. However, relatively low biomass with short incubation time allows us to assume that the change in the carbonate chemistry of the bottles during the incubation period is small.

2.3 Chemical and biological analyses

Chl *a* concentration was measured with the Turner Design 10-AU fluorometer (Welschmeyer, 1994). The net specific growth rate of phytoplankton was calculated from the linear regression between the time (day) and the natural log of Chl *a* concentrations using the data before nutrient depletions. The nutrients and iron concentrations were measured using a QuAAtro-2 continuous flow analyzer (Bran + Luebbe, SPX Corp.) and by flow-injection method with chemiluminescence detection (Obata et al., 1993), respectively. Our Fe measurement method was carefully assessed using SAFe (Sampling and Analysis of Fe) cruise reference standard seawater for an inter-comparison study distributed by the Moss Landing Marine Laboratory and

BGD
10, 4331–4365, 2013

University of California Santa Cruz. We measured $0.10 \pm 0.010\,\mathrm{nmol\,L^{-1}}$ ($n = 3$) and $0.99 \pm 0.023\,\mathrm{nmol\,L^{-1}}$ ($n = 3$) D-Fe by our method, respectively for concentrations of $0.094 \pm 0.008\,\mathrm{nmol\,L^{-1}}$ (S) and $0.923 \pm 0.029\,\mathrm{nmol\,L^{-1}}$ (D2) D-Fe (www.geotraces.org) for the reference standard seawater. Filter samples for POC and PN were freeze-dried followed by exposing HCl fumes overnight to remove inorganic carbon, and these concentrations were measured by CHN analyzer (Perkin Elmer Inc.). For BSi analysis, filter sample was digested by heating to 85 °C for 2 h in a 0.5 % Na_2CO_3 solution (Paasche, 1980). After being neutralized with $0.5\,\mathrm{mol\,L^{-1}}$ HCl, the silicic acid concentration was measured using a QuAAtro-2 continuous flow analyzer. All data for POC, PN, and BSi concentrations were corrected by subtracting appropriate filter blanks. The elemental compositions (POC : PN (hereafter C : N), BSi : PN (Si : N), BSi : POC (Si : C)) of phytoplankton produced during the experiment were calculated by subtracting the value of the beginning of the experiment from the value of the day before nutrient depletions. DIC and TA were measured by the potentiometric Gran plot method with dilute HCl ($0.1000\,\mathrm{mol\,L^{-1}}$; Wako Co. Ltd.) using total alkalinity analyzer (Kimoto Electric Co., Ltd.) according to the method of Edmond (1970). The stability of the titration analysis was checked by DIC reference material (KANSO Co., Ltd., Osaka, Japan), whereby the DIC value was traceable to the certified reference material supplied by Andrew Dickson at University of California, San Diego. The analytical errors were < 0.1 % for both DIC ($\sim 1.1\,\mathrm{\mu mol\,kg^{-1}}$) and TA ($\sim 1.4\,\mathrm{\mu mol\,kg^{-1}}$). pH (total scale) and pCO_2 values were calculated from DIC and TA data using CO2SYS program (Lewis and Wallance, 1998). For microscopic analysis, an adequate volume of fixed seawater was poured into a settling chamber and was allowed to settle for at least 24 h before identification using a phase contrast inverted microscope (Hasle, 1978). Diatom species were identified according to Hasle and Syvertsen (1997). Cell volume of the dominant diatom species was measured as described by Hillebrand et al. (1999), and the cell volume was converted to carbon biomass as reported by Menden-Deuer and Lessard (2000). For F_v/F_m measurement, seawater samples were stored for 15 min in a bench-top incubator at 8 °C in the dark. F_v/F_m values were measured with the Fluorescence

BGD
10, 4331–4365, 2013

Induction and Relaxation (FIRe) system (Satlantic Inc.), in which a blue (455 nm with 60 nm bandwidth) light-emitted diode was incorporated for excitation. The FIRe protocol involved single-turnover flashes within 80 µs duration. Triplicate samples were measured with 10 iterations per sample. The background fluorescence was also measured and subtracted from the sample values using 0.2 µm filtered seawater (Gorbunov and Falkowski, 2004). Raw data were collected following the manufacture's protocol and processed using the Fireworx program for MATLAB software, developed by Audrey B. Barnett (Dalhousie University) for obtaining F_v/F_m values. The PDMPO-stained samples were observed by epifluorescence microscope (Olympus Corp.), and the picture was taken by digital camera (Olympus Corp.). The fluorescence intensity of PDMPO-stained diatom frustule was measured using digital image with Image-Pro Plus software (Media Cybernetics Inc.). During the epifluorescence microscope observation, we used 6 % ND filter to minimize the decay of fluorescence, and the ND filter was removed only when taking pictures.

3 Results

3.1 Experimental conditions

At the beginning the experiment, the nutrient concentrations were $18.1 \pm 0.1\,\mu mol\,L^{-1}$ $NO_3^- + NO_2^-$, $0.64 \pm 0.2\,\mu mol\,L^{-1}$ NH_4^+, $1.47 \pm 0.01\,\mu mol\,L^{-1}$ PO_4^{3-}, and $17.0 \pm 0.1\,\mu mol\,L^{-1}$ $Si(OH)_4$ (mean ± 1 SD, $n = 6$). D- and TD-Fe concentrations of the seawater sample were 0.17 and 1.35 $nmol\,L^{-1}$, respectively. The TA, DIC, pH, and pCO_2 of the seawater sample at the beginning of the experiment were $2249 \pm 3.5\,\mu mol\,kg^{-1}$, $2086 \pm 1.6\,\mu mol\,L^{-1}$, 8.06 ± 0.01, and 386 ± 11 µatm, respectively (mean ± 1 SD, $n = 4$). Mean daily photon flux density in the on-deck incubator was $8.7 \pm 3.2\,mol\,photon\,m^{-2}\,day^{-1}$ during the 7 days of the experiment ranging from 4.9 to $13.0\,mol\,photon\,m^{-2}\,day^{-1}$.

During the course of the experiment, manipulation of carbonate chemistry was successfully archived within the first 2 days by the xCO_2-controlled air bubbling, but the

BGD
10, 4331–4365, 2013

conditions were gradually changed with incubation time in the Fe-added treatments (Fig. 2). The mean pH and pCO_2 during 2 to 6 day period in the C-380 and C-600 treatments were 8.09 ± 0.03 and 356 ± 28 µatm, and 7.88 ± 0.02 and 602 ± 25 µatm, respectively. In the Fe-added treatment, the increase in pH and the decrease in pCO_2 were observed at all CO_2 manipulation treatments due to the intensive phytoplankton production in the bottles (Fig. 2b, d). At the end of the incubations, TD-Fe concentrations in the C-380, C-600, Fe-180, Fe-380, Fe-600, and Fe-1000 media were 0.27 ± 0.02, 0.29 ± 0.04, 4.60 ± 0.16, 4.48 ± 0.10, 4.34 ± 0.06, and 4.18 ± 0.20, respectively (mean ± 1 SD of triplicate incubation bottles), and the concentrations did not differ significantly between C-380 and C-600 treatments, and among the Fe-added treatments. Therefore, we successfully conducted the experiments without inadvertent iron contaminations in the control treatments and Fe-added treatments.

3.2 Phytoplankton growth

In the control conditions, net specific growth rate of both size fractions was significantly higher in the C-380 treatment (> 10 µm: $0.31 \pm 0.02\ d^{-1}$ (mean ± 95 % CL of regression), GF/F-10 µm: $0.13 \pm 0.03\ d^{-1}$) compared to that in the C-600 treatment (> 10 µm: $0.28 \pm 0.03\ d^{-1}$, GF/F-10 µm: $0.06 \pm 0.01\ d^{-1}$) (> 10 µm: $p = 0.011$, GF/F-10 µm: $p = 0.047$; ANOVA) (Fig. 3a, c). In the Fe-added treatments, net specific growth rate was higher than that in the controls without statistically significant difference among CO_2 levels, ranging 0.82 ± 0.05 to $0.92 \pm 0.04\ d^{-1}$ for the > 10 µm fraction and 0.43 ± 0.03 to $0.52 \pm 0.03\ d^{-1}$ for the GF/F-10 µm fraction (Fig. 3b, d). The total Chl *a* concentrations in the Fe-600 and Fe-1000 treatments on day 5 were lower relative to the Fe-180 and Fe-380 treatment (Fig. 3f), although the difference was not affected significantly on the net specific growth rate. These trends in total Chl *a* concentrations were almost identical to that of the large fraction of Chl *a* because of the high dominance (>∼ 90 %) of the large-sized Chl *a* (Fig. 3e, f).

The F_v/F_m in the controls decreased with incubation time, and the values on days 2 and 4 in the C-600 treatment were significantly small compared to that of C-380

BGD
10, 4331–4365, 2013

treatment (day 2: $p < 0.01$; day 4: $p = 0.012$, ANOVA) (Fig. 4a). In the Fe-added treatments, the F_v/F_m values increased from 0.35 (day 0) to ~ 0.55 during the first 3 days followed by the slight decrease with time without statistically significant variations among CO_2 treatments (Fig. 4b).

At the beginning of the incubation, a microscopically identifiable phytoplankton community in the bottles was dominated by diatoms followed by dinoflagellates (Fig. 5). *Chaetoceros* subgenus *Hyalochaete* spp. prominently increased during the first 2–3 days and dominated ~ 70 % in terms of carbon biomass of the phytoplankton community in all treatments (Fig. 5). Among the *Hyalochaete* spp., *C. compressus/contortus* complex and *C. constrictus* were the dominant species followed by *C. diadema*, *C. brevis/laciniosus* complex, *C. debilis*, *C. radicans*, *C. teres*, *C. curvisetus* and *C. socialis*. After the peak of the *Hyalochaete* spp., *Pseudo-nitzschia* spp. and other centric diatoms such as *Eucampia groenlandica* increased in the controls (Fig. 5a, b). In the Fe-added conditions, *Pseudo-nitzschia* spp., *Chaetoceros* subgenus *Phaeoceros* spp. and Rhizosoleniaceae such as *Rhizosolenia* spp., *Proboscia alata*, and *Dactyliosolen fragilissimus* increased in the lower two CO_2 treatments after day 4 (Fig. 5c, d). In contrast, Rhizosoleniaceae did not show the increase in the dominancy after day 4 in the higher two CO_2 treatments (Fig. 5e, f). Note that most *Hyalochaete* spp. can form resting spores and are considered as coastal species (Hasle and Syvertsen, 1997; Sugie et al., 2010a), although the resting spores were not observed throughout the experiment.

3.3 Nutrient dynamics

In the controls, nutrients remained at the end of incubations except for $Si(OH)_4$ in the C-380 treatment on day 7 (Fig. 6a, c, e, g). The $NO_3^- + NO_2^-$, PO_4^{3-}, and $Si(OH)_4$ drawdowns were smaller in the C-600 treatment than that in the C-380 treatment, which reflects the Chl *a* dynamics (Fig. 3). In the Fe-added treatments, nutrients were

BGD
10, 4331–4365, 2013

exhausted between days 4 and 6 in all CO_2 conditions (Fig. 6b, d, f) except for NH_4^+, which was detectable ($\sim 0.1\,\mu mol\,L^{-1}$) at the end of the incubations (Fig. 6h).

We calculated nutrient drawdown per unit Chl *a* increase before nutrient depletions as an index of nutrient requirement per unit phytoplankton biomass (Fig. 7). The $(NO_3^- + NO_2^-)$/Chl *a* in the C-380 treatment was significantly higher than that in the C-600 treatment, whereas no significant change was observed among CO_2 variations in the Fe-added treatments ($p < 0.01$, Dunnett's *t* test). In the Fe-added treatment, PO_4^{3-}/Chl *a* and $Si(OH)_4$/Chl *a* showed a similar trend with that of $(NO_3^- + NO_2^-)$/Chl *a* that no significant change was detected due to CO_2 variations. The nutrient drawdown per unit Chl *a* values in the controls was higher than that of Fe-added treatments ($p < 0.01$, Dunnett's *t* test) probably due to an increase in Chl *a* quota of phytoplankton in the Fe-added treatments (Raven, et al., 1999; Sugie et al., 2011).

3.4 PDMPO fluorescence of the frustule

The Chl *a* concentrations at the end of the PDMPO incubation closely followed those in the 12 L incubation bottles, suggesting the environmental conditions, especially iron availability, were unaltered after dispensed into the 170 mL of PDMPO incubation bottles (Fig. 3e, f). In the control conditions, the fluorescence intensity of the PDMPO in the frustule did not change between C-380 and C-600 treatment except for *Fragilariopsis* spp., which showed 14 % decrease of the fluorescence with increasing CO_2 levels (Fig. 8, Supplement tables). In the Fe-added treatments, we did not measure consistent CO_2-dependent trends in the PDMPO fluorescence, but the values in *C. brevis*/*laciniosus* complex, *C. debilis*, *Pseudo-nitzschia* spp., and *Fragilariopsis* spp. showed decreasing trends with increasing CO_2 concentrations (Fig. 8). The fluorescence values of *Neodenticula seminae* were about two times higher than those of the other species, but no consistent trends against CO_2 variations and iron additions were detected. In general, change in the fluorescence intensities among all treated conditions for the dominant species was small (several percent), but the value of a few minor

BGD
10, 4331–4365, 2013

dominant species changed by 16 % (*C. brevis/laciniosus* complex and *C. debilis*) and ~ 25 % (*Pseudo-nitzschia* spp. and *Fragilariopsis* spp.) (Fig. 5).

3.5 Elemental compositions

To calculate elemental composition, we subtracted the values of particulate matter concentrations from day 5 to day 0 for Fe-limited controls and from day 4 to day 0 for Fe-added treatments, when the nutrients were not exhausted (Fig. 6). The C : N did not change significantly due to the CO_2 variations and iron additions (Fig. 9a). The Si : N in the Fe-limited controls increased 40 % in response to an increase in CO_2 level, whereas the ratio did not change due to the CO_2 variations in the Fe-added treatments (Fig. 9b). Similarly, the Si : C increased significantly in the C-600 treatment compared to that in the C-380 treatment, and did not show a significant variation in the Fe-added treatments (Fig. 9c). The Si : N and Si : C ratios decreased due to the addition of iron (Fig. 9b, c). Nutrient drawdown ratio of $Si(OH)_4 : (NO_3^- + NO_2^-)$ showed the same trend as observed in the elemental composition of particulate matter (data not shown). The $(NO_3^- + NO_2^-) : PO_4^{3-}$ drawdown ratio showed a significant increase in the Fe-added treatments compared to the controls. In the controls, the $(NO_3^- + NO_2^-) : PO_4^{3-}$ drawdown ratio in the C-600 treatment (12.0 ± 0.3 mol : mol) was smaller than that in the C-380 treatment (13.5 ± 0.2 mol : mol), whereas the values did not change due to CO_2 variations in the Fe-added treatments (16.3–16.8 mol : mol).

4 Discussion

We observed relatively high Chl *a* ($\sim 2\,\mu g\,L^{-1}$) with the dominance of coastal, resting spore-forming diatom species throughout the course of the experiment. Temperature, mixed layer depth, and macronutrient concentrations we measured were similar to those reported previously (Fujishima et al., 2001; Leblanc et al., 2005; Onodera and Takahashi, 2009). Karohji (1972) and Martin and Tortell (2006) found coastal centric

BGD
10, 4331–4365, 2013

diatom species as a dominant diatom group in the eastern Bering Sea shelf, whereas pennate diatoms and oceanic centric diatoms such as *Phaeoceros* spp. were found around the central Bering Sea basin. D-Fe concentrations in the present study were intermediate among previous studies that measured in the Bering Sea basin (0.3–0.78 nmol L^{-1}: Fujishima et al., 2001; 0.04–0.10 nmol L^{-1}: Leblanc et al., 2005; 0.1–0.3 nmol L^{-1}: Takata et al., 2005; 0.01 nmol L^{-1}: Buck and Bruland, 2007). In contrast, TD-Fe concentrations at the beginning of this study (1.35 nmol L^{-1}) were higher than previously reported values ($\leq$ 0.4 nmol L^{-1}: Suzuki et al., 2002; Takata et al., 2005). In general, TD-Fe concentrations were higher in the coastal region compared to the oceanic region (e.g., Johnson et al., 1999). The presence of coastal diatom species with high TD-Fe concentrations indicates recent intrusion of the coastal seawater mass before the experiment probably coming from the Aleutian trenches (Mordy et al., 2005; Stabeno et al., 2005). Such a Fe-limited ecosystem with coastal phytoplankton species can often be seen around the coastal to oceanic boundaries such as in the subarctic North Pacific (Sugie et al., 2010a,b). In the Bering Sea basin, the resting spores of the *Hyalochaete* spp. were frequently observed as dominant phytoplankton groups in the mooring sediment trap, close to our experimental site (53.5° N, 177° W; Takahashi et al., 2002). However, there have been no reports concerning the effects of CO_2 and iron on a Fe-limited phytoplankton community with the dominance of coastal diatom species.

4.1 Synergistic effects of CO_2 and iron on phytoplankton dynamics

The addition of iron stimulates the net specific growth rate and increases F_v/F_m values indicating that the phytoplankton community in the control conditions was Fe-limited. Suzuki et al. (2002) also observed low F_v/F_m values with low TD-Fe concentrations in the Bering Sea basin during early summer 1999. It is known that iron or nitrogen limitations lead to a decrease in F_v/F_m (e.g., Greene et al., 1992; Suzuki et al., 2002). Further, in the Fe-limited control conditions, significantly high specific growth rate and F_v/F_m values of phytoplankton in the C-380 compared to those in the C-600 treatment

BGD
10, 4331–4365, 2013

indicate that the phytoplankton community in the C-600 treatment was more severely iron-limited than that in the C-380 treatment. Note that the TD-Fe concentrations did not show a significant change between the two control treatments at the end of the incubations. A recent study reported that the iron bioavailability decreases with decreasing pH in seawater through increasing the conditional stability constant of natural iron-ligand complex (Shi et al., 2010), which strongly supports our observations in the control treatments. In addition, the changes in the net specific growth rate and F_v/F_m values in the controls were observed soon after the change in carbonate chemistry in the media. Such a rapid response to the environmental conditions suggests that the principal effect is caused by the change in iron bioavailability of the seawater medium rather than by physiological acclimation of phytoplankton (Xu et al., 2012).

In the Fe-added treatments, we found insignificant difference in net specific growth rate in terms of Chl *a* and F_v/F_m values among the different CO_2 levels. Previous studies have reported that the net growth rates of some phytoplankton species were influenced by the change in CO_2 levels, whereas the net growth rate of the phytoplankton community in terms of Chl *a* was rarely affected due to CO_2 variations under iron-replete conditions (Kim et al., 2006; Feng et al., 2009, 2010). In addition, Hopkinson et al. (2010) and Endo et al. (2013) reported that F_v/F_m values did not show a significant difference due to variations in CO_2 levels under iron-replete conditions as observed in the present study. This indicates that the photochemistry of PS II is little affected by CO_2 availability under iron-replete conditions. We suggest that the large input of dissolved inorganic iron may cancel out the effect of the modification of iron bioavailability due to the CO_2 variations in the Fe-added treatments. Therefore, the effect of CO_2 on the phytoplankton dynamics was small during their exponential growth phase under iron-replete conditions.

However, we found that the phytoplankton community of the minor dominant species changed slightly with the change in the CO_2 levels in the Fe-added treatments after day 4 when the nutrients were exhausted (Fig. 5). In contrast, in the Fe-limited control conditions, phytoplankton community composition did not change due to the

BGD
10, 4331–4365, 2013

CO_2 variations. Martin and Tortell (2006) and Hopkinson et al. (2010) reported that the phytoplankton community composition did not change due to CO_2 variations under nutrient-replete conditions. The possible difference of the results among the studies may be derived from nutrient conditions. In the present study, the phytoplankton community in the Fe-added treatments also did not change in response to the CO_2 variations before nutrient depletions as reported previously (Martin and Tortell, 2006; Hopkinson et al., 2010). Although the effect of increasing CO_2 levels on the growth rate of phytoplankton is beneficial for some phytoplankton species (e.g., Kim et al., 2006; Hutchins et al., 2009), the net specific growth rate of the diatoms observed in the present study may not be influenced in response to the change in CO_2 levels. Therefore, we conclude that the increase in CO_2 level affects the species composition of phytoplankton under Fe-replete but nutrient-depleted conditions.

4.2 Synergistic effects of CO_2 and iron on elemental composition of plankton community

This study demonstrated for the first time that the Si : N and S : C ratio of the Fe-limited phytoplankton community increased significantly with an increase in CO_2 level. Possible mechanisms underlying the increase in Si : N and Si : C ratios of the diatoms are the increase in silicification, the decrease in cellular N and C content of the diatoms due to decreasing iron, nitrate and light availability (Takeda, 1998; Saito and Tsuda, 2003; Marchetti and Harrison, 2007; Sugie et al., 2010a), and ambient high $Si(OH)_4$ concentration or high $Si(OH)_4$ to NO_3^- ratio (Kudo, 2003; Finkel et al., 2010). In the present study, light conditions were the same among all treatments. Ambient $Si(OH)_4$ to NO_3^- ratio was lower in the C-600 treatment compared to that in the C-380 treatment because of the higher Si : N ratio of the particles in the C-600 treatment than that in the C-380 treatment. According to the result of PDMPO incubations and $Si(OH)_4$/Chl *a* values, the silicon content of the diatom frustules of the dominant species was not changed markedly in response to different experimental conditions. The data of $(NO_3^- + NO_2^-)$/Chl *a* in the Fe-limited controls indicate that the high Si : N ratio under

BGD
10, 4331–4365, 2013

the high-CO_2 conditions was mainly caused by the decrease in cellular N concentrations of the phytoplankton. Furthermore, the phytoplankton community in the C-600 treatment would be more severely Fe-limited compared to that in the C-380 treatment as described above. This leads the phytoplankton in the C-600 conditions to the decrease in Chl *a* quota (e.g., Sugie et al., 2011); then the difference in the $NO_3^- + NO_2^-$ consumption per unit phytoplankton biomass may be large compared to the measured difference in $(NO_3^- + NO_2^-)$/Chl *a* values between C-380 and C-600 treatments. Previous studies reported that the C : N ratio of the diatoms rarely affected the variations in CO_2 levels (Burkhardt et al., 1997, 1999; King et al., 2011; Sun et al., 2011; Sugie and Yoshimura, 2013). It suggests that the C content of the phytoplankton also decreased with increasing CO_2 under Fe-limited conditions, leading to an increase in Si : C ratio in the C-600 treatment. Because N and C assimilations were strongly suppressed against the decrease in iron availability (e.g., Raven et al., 1999), we concluded that the high Si : N and Si : C values in high CO_2 under Fe-limited conditions were derived from the decrease in iron bioavailability, similarly to the difference observed between the Fe-limited controls and the Fe-added treatments.

The nutrient consumption ratio in the previous field CO_2 manipulation studies did not show a significant change in response to the CO_2 variations, most of which were conducted with the addition of dissolved inorganic iron (Bering Sea: Martin and Tortell, 2006; North Atlantic: Feng et al., 2009). Therefore, it is important to note that the nutrient drawdown and elemental composition of the particulate matter in the natural phytoplankton communities should be examined under (iron) unamended seawater to forecast the future nutrient biogeochemistry, because iron and nutrient addition potentially alter the community response against the ambient environment. Unfortunately, we have very little data available concerning the effect of CO_2 on the Fe-limited natural phytoplankton community. Our recent study reported that no significant change was observed in the Si : N drawdown ratio of the oceanic diatom-dominated phytoplankton community in the Bering Sea, central and western subarctic Pacific regions, which were conducted during the summer in 2007 and 2008, respectively (Endo et al., 2013;

BGD
10, 4331–4365, 2013

Yoshimura et al., 2013). As far as we can consider, the factors producing such discrepancies in the Si : N ratio are follows: (i) the difference of the phytoplankton communities; (ii) non-linear response of the Si : N ratio of the diatoms, which depends on their iron nutritional status (Bucciarelli et al., 2010); and/or (iii) difference of the iron-binding ligand, which would differ in the dissociation behavior of bioavailable iron from natural iron-ligand complex in response to the change in CO_2 levels (Shi et al., 2010). Further study is apparently needed to clarify the synergistic effects of CO_2 and iron on the nutrient stoichiometry of phytoplankton under Fe-limited ecosystems to better understand the ocean biogeochemistry in the future high-CO_2 oceans.

4.3 Implications on nutrient biogeochemistry for the future high-CO_2 oceans

The present study is the first demonstration that high CO_2 affects nutrient dynamics on Fe-limited phytoplankton communities. The high Si : N and Si : C values under the high-CO_2 conditions in the Fe-limited controls probably derived from the further Fe limitation of coastal diatoms due to the decrease in iron bioavailability. Recent studies indicated that the iron bioavailability and iron distribution will change in future high CO_2 oceans (Mahowald et al., 2009; Millero et al., 2009; Shi et al., 2010); however, there is very limited information available to date on whether the iron availability will increase or not in the future. Our results indicate that iron bioavailability will decrease under the future high-CO_2 conditions in the oceanic to coastal boundary regions. We suggest that the modulation of the iron bioavailability under the future high-CO_2 conditions is one of the key factors controlling oceanic nutrient biogeochemistry.

The high Si : N and Si : C ratios were derived from the decrease in cellular N and C content of the phytoplankton in the present study. This result indicates that the effect of biological carbon pump associated with diatom (Tréguer and Pondaven, 2000) will decrease under high-CO_2 conditions. In the PDMPO incubation experiment, when the nutrient remained in conditions, the silicification of a few minor diatom species decreased with increasing CO_2 levels, suggesting that the frustule thickness of some diatom species decreased with increasing CO_2 levels (Fig. 8). A previous study reported

BGD
10, 4331–4365, 2013

that the dissolution rate of diatom frustule using *Thalassiosira weissflogii* was enhanced due to an increase in CO_2 level (Milligan et al., 2004). The Si concentration per unit surface area of the diatom *Pseudo-nitzschia pseudodelicatissima* also decreased with increasing CO_2 levels from ~ 200 to ~ 750 µatm under various dissolved inorganic iron hydroxide concentrations (Sugie and Yoshimura, 2013). These studies suggest that the silicification of some diatom species can be influenced in response to the change in ambient CO_2 levels. There is increasing evidence that the responses of the phytoplankton to the high-CO_2 conditions are often species- and strain-specific (e.g., Langer et al., 2009; Hutchins et al., 2009). In addition, the low silicon content of diatom cells with low N and C content will be easily remineralized in the upper water column. Because diatom frustule is considered as one of the most influential ballast minerals, carrying organic soft tissues to the deep ocean (Passow and De La Rocha, 2006), fast dissolution of diatomaceous Si with low N and C content causes further decrease in the effect of biological pump under the future high CO_2 conditions. Therefore, the community composition of diatoms is critical when considering the effect of CO_2 on the biogeochemical cycling of nutrients in the surface ocean. The elemental composition and particulate property of each diatom species are important parameters for predicting the future biogeochemical cycling of nutrients in the oceans.

Supplementary material related to this article is available online at: http://www.biogeosciences-discuss.net/10/4331/2013/bgd-10-4331-2013-supplement.pdf.

Acknowledgements. We thank A. Matsuoka of CERES Inc. for analyzing POC and PN and A. Murayama of Hokkaido Univ. for analyzing iron samples. This work was conducted in the framework of the Plankton Ecosystem Response to CO_2 Manipulation Study (PERCOM) project and supported by the grants from CRIEPI (#090313) and Grants-in-Aid for Scientific Research (#22681004).

BGD
10, 4331–4365, 2013

References

Arrigo, K. R., Robinson, D. H., Worthen, D. L., Dunbar, R. B., DiTullio, G. R., VanWoert, M., and Lizotte, M. P.: Phytoplankton community structure and the drawdown of nutrients and CO_2 in the Southern Ocean, Science, 283, 365–367, 1999.

Bucciarelli, E., Pondaven, P., and Sarthou, G.: Effects of an iron-light co-limitation on the elemental composition (Si, C, N) of the marine diatoms *Thalassiosira oceanica* and *Ditylum brightwellii*, Biogeosciences, 7, 657–669, doi:10.5194/bg-7-657-2010, 2010.

Buck, K. N. and Bruland, K. W.: The physicochemical speciation of dissolved iron in the Bering Sea, Alaska. Limnol. Oceanogr., 52, 1800–1808, 2007.

Burkhardt, S. and Riebesell, U.: CO_2 availability affects elemental composition (C : N : P) of the marine diatom *Skeletonema costatum*, Mar. Ecol. Prog. Ser., 155, 67–76, 1997.

Burkhardt, S., Zondervan, I., and Riebesell, U.: Effect of CO_2 concentration on C : N : P ratio in marine phytoplankton: a species comparison, Limnol. Oceanogr., 44, 683–690, 1999.

Caldeira, K. and Wickett, M. E.: Ocean model predictions of chemistry changes from carbon dioxide emissions to the atmosphere and ocean, J. Geophys. Res., 110, C09S04, doi:10.1029/2004JC002671, 2005.

de Baar, H. J. W., Boyd, P. W., Coale, K. H., Landry, M. R., Tsuda, A., Assmy, P., Bakker, D. C. E., Bozec, Y., Barber, R. T., Brzezinski, M. A., Buesseler, K. O., Boyé, M., Croot, P. L., Gervais, F., Gorbunov, Y., Harrison, P. J., Hiscock, W. T., Laan, P., Lancelot, C., Law, C. S., Levasseur, M., Marchetti, A., Millero, F. J., Nishioka, J., Nojiri, Y., van Oijen, T., Riebesell, U., Rijkenberg, M. J. A., Saito, H., Takeda, S., Timmermans, K. R., Veldhuis, M. J. W., Waite, A. M., and Wong, C. S.: Synthesis of iron fertilization experiments: from the Iron Age in the Age of Enlightenment, J. Geophys. Res., 110, C09S16, doi:10.1029/2004JC002601, 2005.

Edmond, J. W.: High precision determination of titration alkalinity and total carbon dioxide content of seawater by potentiometric titration, Deep-Sea Res., 17, 737–750, 1970.

Endo, H., Yoshimura, T., Kataoka, T., and Suzuki, K.: Effects of CO_2 and iron availability on phytoplankton and eubacterial community compositions in the northwest subarctic Pacific, J. Exp. Mar. Biol. Ecol., 439, 160–175, 2013.

Feng, Y., Hare, C. E., Leblanc, K., Rose, J. M., Zhang, Y., DiTullio, G. R., Lee, P. A., Wilhelm, S. W., Rowe, J. M., Sun, J., Nemcek, N., Gueguen, C., Passow, U., Benner, I., Brown, C., and Hutchins, D. A.: Effects of increased pCO_2 and temperature on the North

BGD
10, 4331–4365, 2013

Atlantic spring bloom, I. The phytoplankton community and biogeochemical response, Mar. Ecol. Prog. Ser., 388, 13–25, 2009.
Feng, Y., Hare, C. E., Rose, J. M., Handy, S. M., DiTullio, G. R., Lee, P. A., Smith Jr., W. O., Peloquin, J., Tozzi, S., Sun, J., Zhang, Y., Dunbar, R. B., Long, M. C., Sohst, B., Lohan, M., and Hutchins, D. A.: Interactive effects of iron, irradiance and CO_2 on Ross Sea phytoplankton, Deep-Sea Res. Pt. I, 57, 368–83, 2010.
Finkel, Z. V., Matheson, K. A., Regan, K. S., and Irwin, A. J.: Genotypic and phenotypic variation in diatom silicification under paleo-oceanographic conditions, Geobiology, 8, 433–445, 2010.
Fujishima, Y., Ueda, K., Maruo, M., Nakayama, E., Tokutome, C., Hasegawa, H., Matsui, M., and Sohrin, Y.: Distribution of trace bioelements in the subarctic north Pacific Ocean and the Bering Sea (the R/V *Hakuho Maru* cruise KH-97-2), J. Oceanogr., 57, 261–273, 2001.
Gorbunov, M. Y. and Falkowski, P. G.: Fluorescence induction and relaxation (FIRe) technique and instrumentation for monitoring photosynthetic processes and primary production in aquatic ecosystems, in: Photosynthesis. Fundamental Aspects to Global Perspectives, edited by: Bruce, D. and van der Est, A., Allen Press, Montreal, 1029–1031, 2004.
Greene, R. M., Geider, R. J., Kolber, Z., and Falkowski, P. G.: Iron-induced changes in light harvesting and photochemical energy conversion processes in eukaryotic algae, Plant Physiol., 100, 565–575, 1992.
Hasle, G. R.: Using the inverted microscope, in: Phytoplankton Manual, edited by: Sourina, A., UNESCO, Paris, 191–196, 1978.
Hasle, G. R. and Syvertsen, E. E.: Marine diatoms, in: Identifying Marine Phytoplankton, edited by: Tomas, C. R., Academic Press, London, 5–385, 1997.
Hillebrand, H., Durseien, C. D., Kirschtel, D., Pollingher, U., and Zohary, T.: Biovolume calculation for pelagic and benthic microalgae, J. Phycol., 35, 403–424, 1999.
Hopkinson, B. M., Xu, Y., Shi, D., McGinn, P. J., and Morel, F. M. M.: The effect of CO_2 on the photosynthetic physiology of phytoplankton in the Gulf of Alaska, Limnol. Oceanogr., 55, 2011–2024, 2010.
Hutchins, D. A., Mulholland, M. R., and Fu, F. X.: Nutrient cycles and marine microbes in a CO_2-enriched ocean, Oceanography, 22, 128–145, 2009.
Ichinomiya, M., Gomi, Y., Nakamachi, M., Ota, T., and Kobari, T.: Temporal patterns in silica deposition among siliceous plankton during the spring bloom in the Oyashio region, Deep-Sea Res. Pt. II, 57, 1665–1670, 2010.

BGD
10, 4331–4365, 2013

Johnson, K. S., Chavez, F. P., and Friederich, G. E.: Continental-shelf sediment as a primary source of iron for coastal phytoplankton, Nature, 398, 697–700, 1999.

Karohji, K.: Regional distribution of phytoplankton in the Bering Sea and western and northern subarctic regions of the North Pacific Ocean in summer, in: Biological Oceanography of the Northern North Pacific Ocean, edited by: Takenouti, A. Y., Idemitsu Shouten, Tokyo, Japan, 99–115, 1972.

Kim, J. M., Lee, K., Shin, K., Kang, J. H., Lee, H. W., Kim, M., Jang, P. G., and Jang, M. C.: The effect of seawater CO_2 concentration on growth of a natural phytoplankton assemblage in a controlled mesocosm experiment, Limnol. Oceanogr., 51, 1629–1636, 2006.

King, A. L., Sañudo-Wilhelmy, S. A., Leblanc, K., Hutchins, D. A., and Fu, F.: CO_2 and vitamin B_{12} interactions determine bioactive trace metal requirements of a subarctic Pacific diatom, ISME J., 5, 1388–1396, 2011.

Kudo, I.: Change in the uptake and cellular Si : N ratio in diatoms responding to the ambient Si : N ratio and growth phase, Mar. Biol., 143, 39–46, 2003.

Langer, G., Nehrke, G., Probert, I., Ly, J., and Ziveri, P.: Strain-specific responses of *Emiliania huxleyi* to changing seawater carbonate chemistry, Biogeosciences, 6, 2637–2646, doi:10.5194/bg-6-2637-2009, 2009.

Leblanc, K. and Hutchins, D. A.: New applications of a biogenic silica deposition fluorophore in the study of oceanic diatoms, Limnol. Oceanogr.-Meth., 3, 462–476, 2005.

Leblanc, K., Hare, C. E., Boyd, P. W., Bruland, K. W., Sohst, B., Pickmere, S., Lohan, M. C., Buck, K., Ellwood, M., and Hutchins, D. A.: Fe and Zn effects on the Si cycle and diatom community structure in two contrasting high and low-silicate HNLC areas, Deep-Sea Res. Pt. I, 52, 1842–1864, 2005.

Lewis, E. and Wallance, D. W. R.: Program developed for CO_2 system calculations, ORNL/CDIAC-105, Carbon dioxide information analysis center, Oak Ridge National Laboratory, US Department of Energy, Oak Ridge, Tennessee, 1998.

Mahowald, N. M., Engelstaedter, S., Luo, C., Sealy, A., Artaxo, P., Benitez-Nelson, C., Bonnet, S., Chen, Y., Chuang, P. Y., Cohen, D. D., Dulac, F., Herut, B., Johansen, A. M., Kubilay, N., Losno, R., Maenhaut, W., Paytan, A., Prospero, J. M., Shank, L. M., and Siefert, R. L.: Atmospheric iron deposition: global distribution, variability, and human perturbations, Annu. Rev. Mar. Sci., 1, 245–278, 2009.

BGD
10, 4331–4365, 2013

Marchetti, A. and Harrison, P. J.: Coupling changes in the cell morphology and the elemental (C, N, and Si) composition of the pennate diatom *Pseudo-nitzschia* due to iron deficiency, Limnol. Oceanogr., 52, 2270–2284, 2007.

Martin, C. L. and Tortell, P. D.: Bicarbonate transport and extracellular carbonic anhydrase activity in Bering Sea phytoplankton assemblages: results from isotope disequilibrium experiments, Limnol. Oceanogr., 51, 2111–2121, 2006.

Menden-Deuer, S. and Lessard, E. J.: Carbon to volume relationships for dinoflagellates, diatoms, and other protist plankton, Limnol. Oceanogr., 45, 569–579, 2000.

Millero, F. J., Woosley, R., DiTrolio, B., and Waters, J.: Effect of ocean acidification on the speciation of metals in seawater, Oceanography, 22, 72–85, 2009.

Milligan, A. J., Varela, D. E., Brzezinski, M. A., and Morel, F. M. M.: Dynamics of silicon metabolism and silicon isotopic discrimination in a marine diatom as a function of pCO_2, Limnol. Oceanogr., 49, 322–329, 2004.

Mordy, C. M., Stabeno, P. J., Ladd, C., Zeeman, S., Wisegarver, D. P., Salo, S. A., and Hunt, G. L.: Nutrients and primary production along the eastern Aleutian Island Archipelago, Fish. Oceanogr., 14, 55–76, 2005.

Obata, H., Karatani, H., and Nakayama, E.: Automated determination of iron in seawater by chelating resin concentration and chemiluminescence detection, Anal. Chem., 65, 1524–1528, 1993.

Onodera, J. and Takahashi, K.: Long-term diatom fluxes in response to oceanographic conditions at Stations AS and SA in the central subarctic Pacific and the Bering Sea, 1990–1998, Deep-Sea Res. Pt. I, 56, 189–211, 2009.

Paasche, E.: Silicon content of five marine plankton diatom species measured with a rapid filter method, Limnol. Oceanogr., 25, 474–480, 1980.

Passow, U. and De La Rocha C. L.: Accumulation of mineral ballast on organic aggregates, Global Biogeochem. Cy., 20, GB1013, doi:10.1029/2005GB002579, 2006.

Raven, J. A., Evans, M. C. W., and Korb, R. E.: The role of trace metals in photosynthetic electron transport in O_2-evolving organisms, Photosynth. Res., 60, 111–149, 1999.

Raven, J., Caldeira, K., Elderfield, H., Hoegh-Guldberg, O., Liss, P., Riebesell, U., Shepherd, J., Turley, C., and Watson, A.: Ocean acidification due to increasing atmospheric carbon dioxide, Royal Society, London, 57 pp., 2005.

Redfield, A. C., Ketchum, B. H., and Richards, F. A.: The influence of organisms on the composition of seawater, in: The Sea, vol. 2, edited by: Hill, M. N., Wiley, New York, 26–77, 1963.

BGD
10, 4331–4365, 2013

Saito, H. and Tsuda, A.: Influence of light intensity on diatom physiology and nutrient dynamics in the Oyashio region, Prog. Oceanogr., 57, 251–263, 2003.
Saito, M. A., Goepfert, T. J., and Ritt, J. T.: Some thoughts on the concept of colimitation: three definitions and the importance of bioavailability, Limnol. Oceanogr., 53, 276–290, 2008.
Shi, D., Xu, Y., Hopkinson, B. M., and Morel, F. M. M.: Effect of ocean acidification on iron availability to marine phytoplankton, Science, 327, 676–679, 2010.
Stabeno, P. J., Kachel, D. G., Kachel, N. B., and Sullivan, M. E.: Observations from mooring in the Aleutian Passes: temperature, salinity and transport, Fish. Oceanogr., 39–54, 2005.
Sugie, K. and Yoshimura, T.: Effects of pCO_2 and iron on the elemental composition and cell geometry of the marine diatom *Pseudo-nitzschia pseudodelicatissima*, J. Phycol., in press, doi:10.1111/jpy.12054, 2013.
Sugie, K., Kuma, K., Fujita, S., and Ikeda, T.: Increase in Si : N drawdown ratio due to resting spore formation by spring bloom-forming diatoms under Fe- and N-limited conditions in the Oyashio region, J. Exp. Mar. Biol. Ecol., 382, 108–116, 2010a.
Sugie, K., Kuma, K., Fujita, S., Nakayama, Y., and Ikeda, T.: Nutrient and diatom dynamics during late winter and spring in the Oyashio region of the western subarctic Pacific Ocean, Deep-Sea Res. Pt. II, 57, 1630–1642, 2010b.
Sugie, K., Kuma, K., Fujita, S., Ushizaka, S., Suzuki, K., and Ikeda, T.: Importance of intracellular Fe pools on growth of marine diatoms by using unialgal cultures and the Oyashio region phytoplankton community during spring, J. Oceanogr., 67, 183–196, 2011.
Sun, J., Hutchins, D. A., Feng, Y., Seubert, E. L., Caron, D. A., and Fu, F. X.: Effects of changing pCO_2 and phosphate availability on domoic acid production and physiology of the marine harmful bloom diatom *Pseudo-nitzschia multiseries*, Limnol. Oceanogr., 56, 829–840, 2011.
Suzuki, K., Liu, H., Saino, T., Obata, H., Takano, M., Okamura, K., Sohrin, Y., and Fujishima, Y.: East-west gradients in the photosynthetic potential of phytoplankton and iron concentration in the subarctic Pacific Ocean during early summer, Limnol. Oceanogr., 47, 1581–1594, 2002.
Suzuki, R. and Ishimaru, T.: An improved method for the determination of phytoplankton chlorophyll using N,N-dimethylformamide, J. Oceanogr. Soc. Jpn., 46, 190–194, 1990.
Takahashi, K., Fujitani, N., and Yanada, M.: Long term monitoring of particulate fluxes in the Bering Sea and the central subarctic Pacific Ocean, 1997–2000, Prog. Oceanogr., 55, 95–112, 2002.

BGD
10, 4331–4365, 2013

Takata, H., Kuma, K., Iwade, S., Isoda, Y., Kuroda, H., and Senjyu, T.: Comparative vertical distributions of iron in the Japan Sea, the Bering Sea, and the western North Pacific Ocean, J. Geophys. Res., 110, C07004, doi:10.1029/2004JC002783, 2005.

Takeda, S.: Influence of iron availability on nutrient consumption ratio of diatoms in oceanic waters, Nature, 393, 774–777, 1998.

Tréguer, P. and Pondaven, P.: Silica control of carbon dioxide, Nature, 406, 358–359, 2000.

Welschmeyer, N. A.: Fluorometric analysis of chlorophyll *a* in the present of chlorophyll *b* and pheopigments, Limnol. Oceanogr., 39, 1985–1992, 1994.

Xu, Y., Shi, D., Aristilde, L., and Morel, F. M. M.: The effect of pH on the uptake of zinc and cadmium in marine phytoplankton: possible role of weak complexes, Limnol. Oceanogr., 57, 293–304, 2012.

Yoshimura, T., Nishioka, J., Suzuki, K., Hattori, H., Kiyosawa, H., and Watanabe, Y. W.: Impacts of elevated CO_2 on organic carbon dynamics in nutrient depleted Okhotsk Sea surface waters, J. Exp. Mar. Biol. Ecol., 395, 191–198, 2010.

Yoshimura, T., Suzuki, K., Kiyosawa, T., Ono, T., Kuma, K., and Nishioka, J.: Impacts of elevated CO_2 on particulate and dissolved organic matter production by the iron deficient plankton ecosystem in subarctic waters, in review, 2013.

BGD
10, 4331–4365, 2013

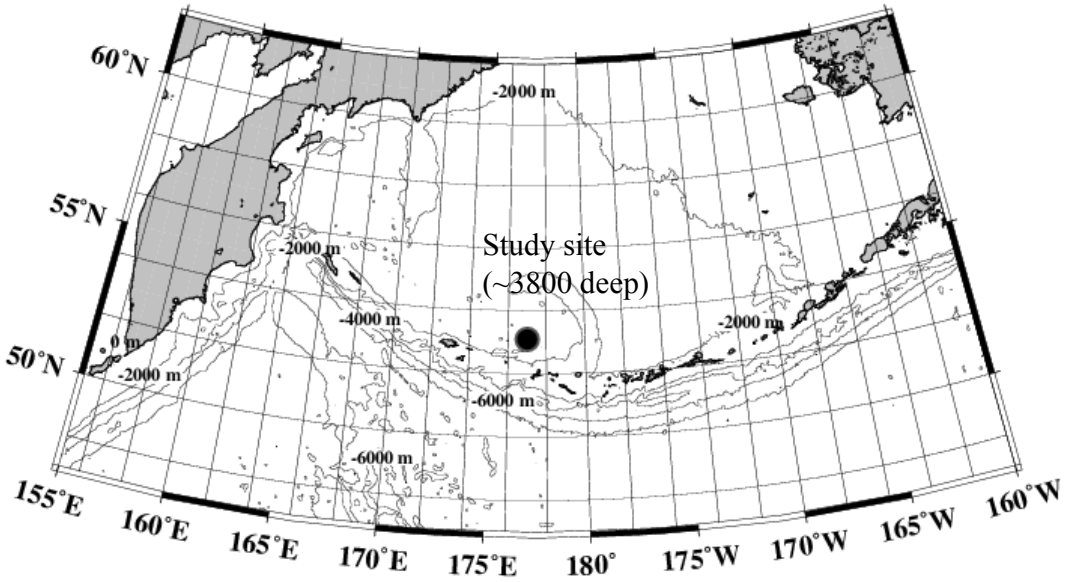

Fig. 1. Sampling location (53° 05′ N, 177° 00′ W) in the Bering Sea basin.

BGD
10, 4331–4365, 2013

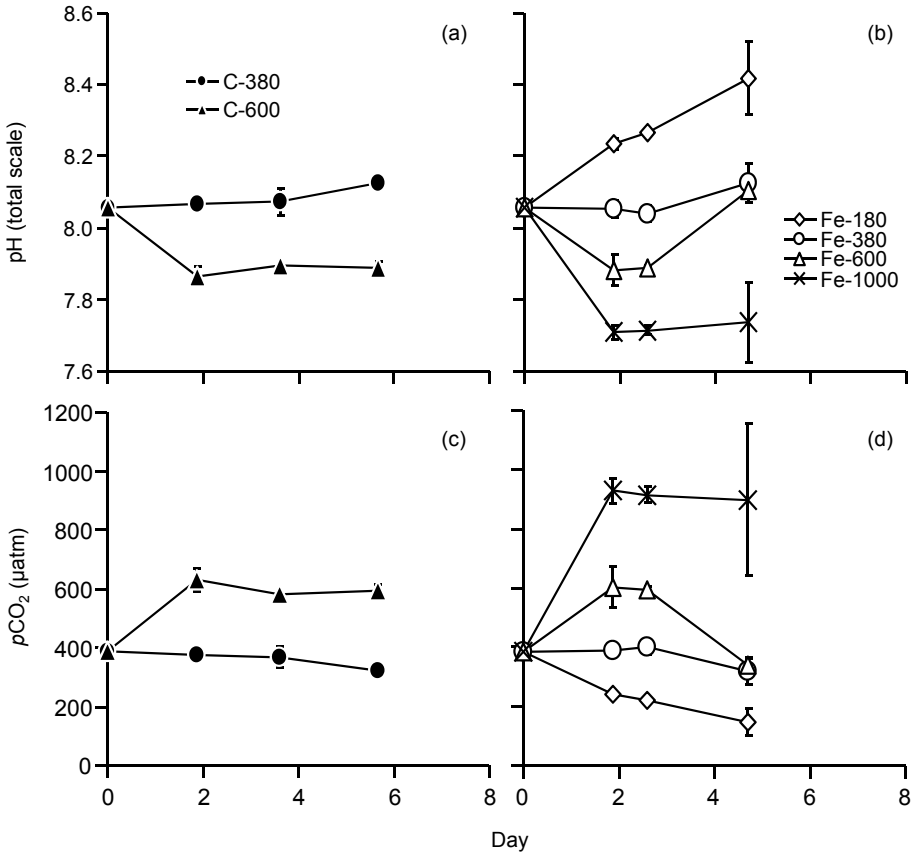

Fig. 2. Temporal change in **(a)** and **(b)** pH (total scale) and **(c)** and **(d)** pCO_2 during the course of incubation experiment. **(a)** and **(c)** are controls. **(b)** and **(d)** are iron-added treatments. Data represent mean ± 1 SD of the triplicate bottles.

BGD
10, 4331–4365, 2013

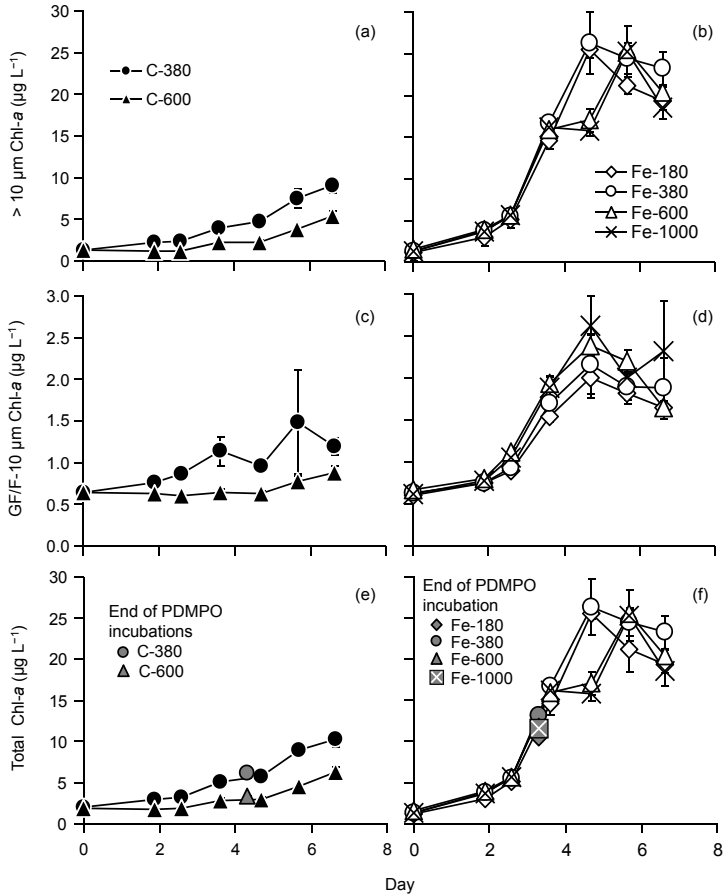

Fig. 3. Temporal change in size fractionated chlorophyll *a* concentrations. **(a)** and **(b)** > 10 µm, **(c)** and **(d)** 10 µm-GF/F (~ 0.7 µm), and **(e)** and **(f)** total concentrations. Left column: controls, right column: iron-added treatments. Data represent mean ± 1 SD of the triplicate bottles.

BGD
10, 4331–4365, 2013

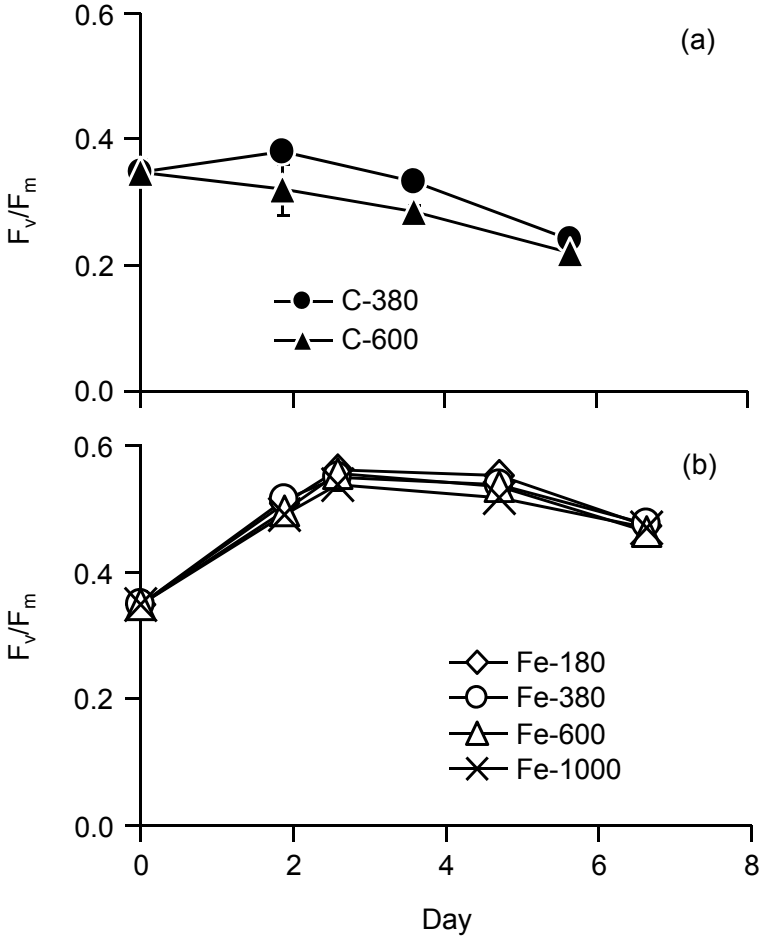

Fig. 4. Temporal change in F_v/F_m values: **(a)** controls and **(b)** iron-added treatments.

BGD
10, 4331–4365, 2013

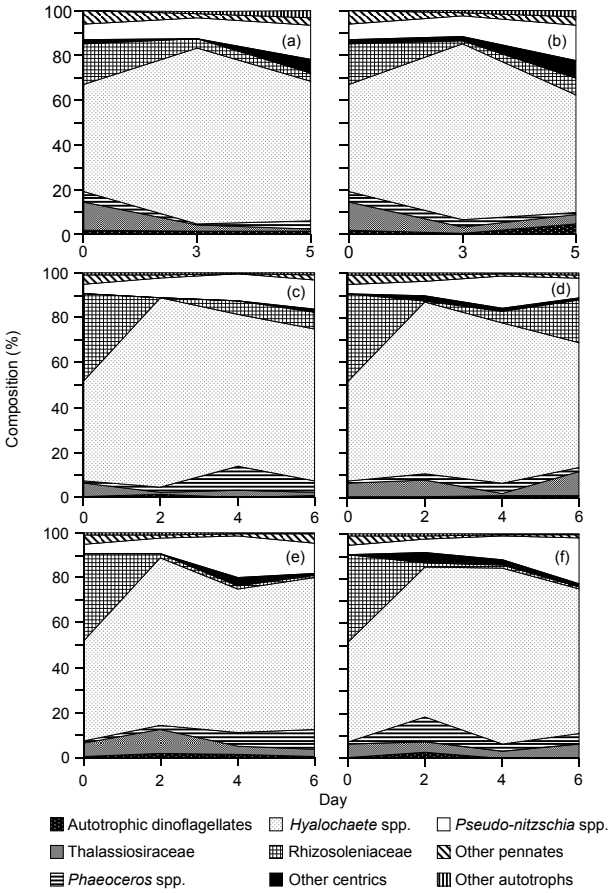

Fig. 5. Temporal change in the species composition of diatoms in terms carbon biomass. **(a)** 380 ppm CO_2 control, **(b)** 600 ppm CO_2 control, **(c)** 180 ppm CO_2 Fe added, **(d)** 380 ppm CO_2 Fe added, **(e)** 600 ppm Fe added and **(f)** 1000 ppm CO_2 Fe-added treatments.

BGD
10, 4331–4365, 2013

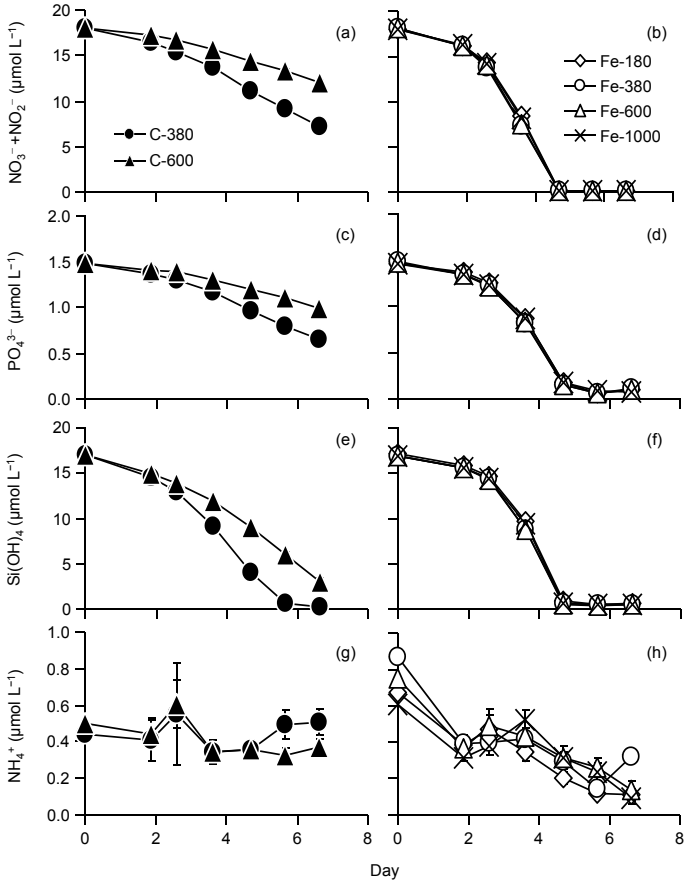

Fig. 6. Temporal change in **(a)** and **(b)** $NO_3^- + NO_2^-$, **(c)** and **(d)** PO_4^{3-}, **(e)** and **(f)** $Si(OH)_4$, and **(g)** and **(h)** NH_4^+ concentrations. Left column: controls, right column: iron-added treatments. Data represent mean ± 1 SD of the triplicate bottles.

BGD
10, 4331–4365, 2013

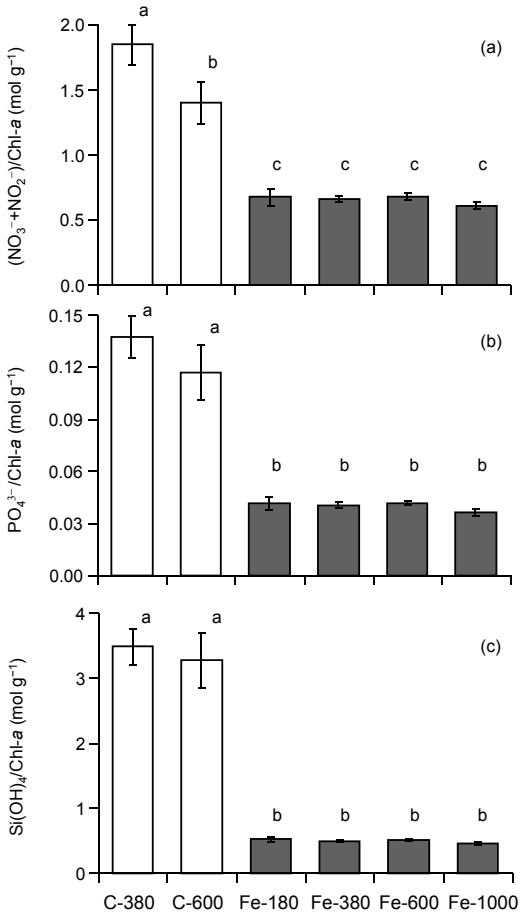

Fig. 7. Comparison of nutrient drawdown per unit chlorophyll *a* (Chl *a*) increase. **(a)** (NO_3^- + NO_2^-)/Chl *a*, **(b)** PO_4^{3-}/Chl *a*, and **(c)** $Si(OH)_4$/Chl *a*. Data represent mean ± 1 SD of the triplicate bottles. Alphabets above the bar represent statistical result of Tukey's B group test.

BGD
10, 4331–4365, 2013

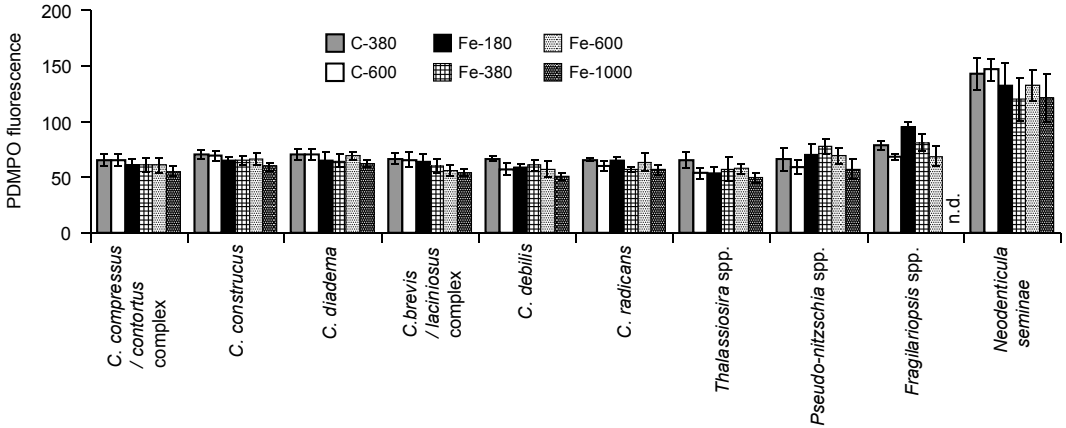

Fig. 8. Fluorescence intensity of the PDMPO-stained frustule of the diatom species. n.d.: not detected. Statistical results are shown in Supplement tables.

BGD
10, 4331–4365, 2013

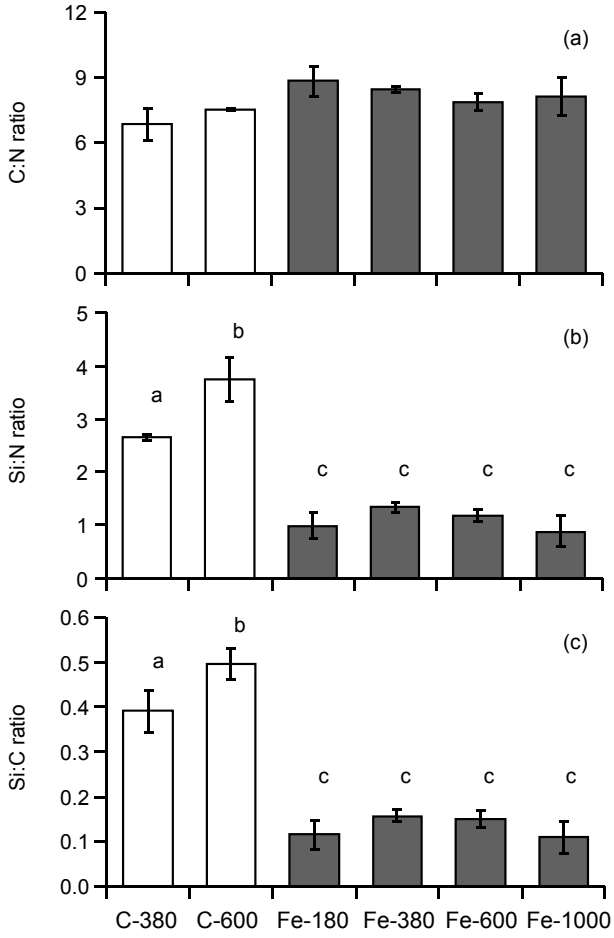

Fig. 9. Comparison of particulate **(a)** C : N, **(b)** Si : N and **(c)** Si : C ratio produced during the experiment. Data represent mean ± 1 SD of the triplicate bottles. Alphabets above the bar represent statistical result of Tukey's B group test.

BGD
10, 4331–4365, 2013